How important is intraseasonal surface wind variability to real-time ENSO prediction?

Wanqiu Wang,[1] Mingyue Chen,[1] Arun Kumar,[1] and Yan Xue[1]

Received 6 April 2011; revised 11 May 2011; accepted 11 May 2011; published 9 July 2011.

[1] Variations with initial time in the prediction of the El Niño–Southern Oscillation (ENSO) are analyzed based on the NCEP operational forecasts. It is found that the forecasted ENSO can be greatly affected by intraseasonal surface wind variability in the western Pacific (WPac), especially that associated with the Madden-Julian Oscillation (MJO). In the model forecasts, Kelvin waves forced by intraseasonal winds in the WPac propagate eastward and reach the eastern Pacific in about 60 days, where the induced surface temperature (SST) anomalies dissipate and expand westward. Differences in the forecasted Nino3.4 SSTs can be 0.5 K or larger depending on the phase and amplitude of the MJO. Variations in WPac surface winds are also found to have impacts on the spread of the forecasted Nino3.4 SSTs. Relevance of these results to the ensemble strategies currently used in the operational climate prediction centers is discussed. **Citation:** Wang, W., M. Chen, A. Kumar, and Y. Xue (2011), How important is intraseasonal surface wind variability to real-time ENSO prediction?, *Geophys. Res. Lett.*, *38*, L13705, doi:10.1029/2011GL047684.

1. Introduction

[2] In this paper the influence of intraseasonal surface wind anomalies on El Niño Southern Oscillation (ENSO) prediction is analyzed. The possible influence of initial intraseasonal surface winds on the ocean state, from which ENSO forecasts using coupled models are initialized, may impart enhanced predictability to ENSO through the ocean memory. On the other hand, since observed intraseasonal events are unlikely to be predicted beyond a short lead-time, and if they are to occur *after* the forecast initialization, they may also impart a level of unpredictability to ENSO, particularly for the prediction of the ENSO amplitude. The latter factor is of special relevance in forecasting the global impacts of ENSO which depend critically on the amplitude of individual events.

[3] An example of the potential influence of initial intraseasonal wind anomalies on ENSO prediction from the coupled Climate Forecast System (CFS) operational at the National Centers for Environmental Prediction (NCEP) is illustrated in Figure 1. Descriptions of the model, forecast data, and details for the analysis procedure are given in section 2. Figure 1c which shows the evolution of Nino3.4 sea surface temperature (SST) anomalies for forecasts initialized from 1 November 2007 to 31 January 2008. This period was characterized by two cycles of a strong Madden-Julian Oscillation (MJO). Consistent with the development of a La Niña event during this period, all forecasts had below-normal SSTs throughout most of the target forecast period. However, the forecasted Nino3.4 SST anomalies varied greatly with initial time. Forecasts from mid November 2007 and early-mid January 2008, corresponding to strong westerly tropical surface 10-meter zonal wind (U_{10m}) anomalies in the western Pacific (Figure 1a), evolved towards near-normal conditions, while forecasts from mid December 2007 and near late January 2008, when tropical easterly U_{10m} anomalies dominated in the western Pacific, produced relative strong La Niña conditions during the entire target period.

[4] Clear variations in the amplitude of the forecasted Nino3.4 SST with initial time are better seen in Figure 1d which shows a substantial *intraseasonal* component with respect to *initial time* (IIT) anomalies with relatively warmer (colder) forecasted Nino3.4 SST anomalies corresponding to tropical intraseasonal westerly (easterly) anomalies in the western Pacific (WPac, 120°E–160°E) (Figure 1b). Absolute differences in Nino3.4 SST for the same target time between strong westerly and easterly phases of WPac zonal winds can be 0.5 K or larger. These results indicate that ENSO forecasts can vary greatly with initial time and the variation may be strongly associated with the initial winds in the western Pacific.

[5] The association of ENSO evolution with westerly wind events (WWEs) has been documented in various previous studies [*Vecchi and Harrison*, 2000; *Zhang and Gottschalck*, 2002]. Most of WWEs are associated with the MJO, although they are also found to be linked with a variety of atmospheric phenomena [*Eisenman et al.*, 2005; *Seiki and Takayabu*, 2007]. WWEs affect the underlying ocean by generating perturbations along the thermocline that result in eastward-propagating Kelvin waves [*Kessler et al.*, 1995; *Hendon et al.*, 1998; *Batstone and Hendon*, 2005; *Seo and Xue*, 2005]. WWEs also cool the western Pacific through changes in the ocean-atmosphere heat flux and upper-ocean mixing, and warm the central-eastern Pacific through zonal advection by the induced eastward current anomalies [*Picaut et al.*, 1996; *Shinoda and Hendon*, 2001; *McPhaden*, 2002, 2008]. *Kessler and Kleeman* [2000] demonstrated the rectification of low-frequency SST anomalies from purely oscillating wind stresses at intraseasonal time scales due to nonlinear dependence of evaporation on surface wind and nonlinearly generated zonal advection and vertical advection. Contributions to ENSO variance by the intraseasonal wind variability can be as large as that by oceanic low-frequency dynamical processes [*McPhaden et al.*, 2006]. Indeed, previous studies have shown that the onset of the 1997/1998 ENSO event was led by several strong MJO associated WWEs and forecast models failed

[1]Climate Prediction Center, NCEP, NWS, NOAA, Camp Springs, Maryland, USA.

0094-8276/11/2011GL047684

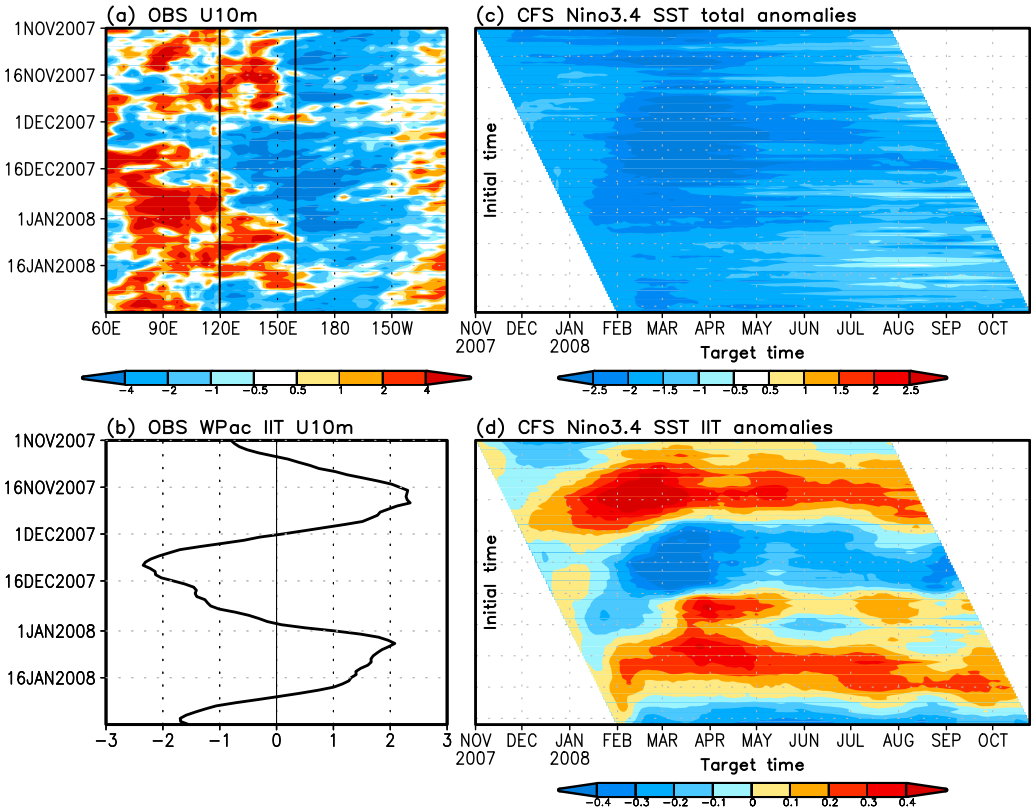

Figure 1. (a) Time-longitude section of observed 5°S–5°N average U_{10m} anomalies, (b) observed intraseasonal WPac (120°E–160°E/5°S–5°N average) U_{10m} anomalies, (c) forecasted total Nino3.4 SST anomalies, and (d) forecasted Nino3.4 SST intraseasonal with respect to initial time (IIT) anomalies.

to predict the strength of this strong event before the impacts of the observed WWEs were included in the initial state of the models [*Barnston et al.*, 1999; *Vitart et al.*, 2003]. It has also been found that the predicted ENSO, for example, the Nino3.4 index, strongly depends on the stochastic perturbations in atmospheric initial conditions [*Shi et al.*, 2009, 2010].

[6] Quantifying the influence of intraseasonal surface wind anomalies based on a longer time-series of ENSO prediction from an initialized coupled forecast system is the theme of this paper. After analyzing the dependence of ENSO prediction on initial surface winds, we also discuss implications for the various alternatives for a forecast system design for seasonal climate predictions.

2. Data and Methods

[7] In this study, we analyze relationship between forecasted ENSO-related SSTs and initial intraseasonal surface wind anomalies based on the forecasts from the NCEP's operational coupled climate forecast system (i.e., the CFS). The unique feature of the CFS is that its real-time forecasts have been initialized from observed atmospheric and oceanic conditions every day after its implementation in late 2004, allowing for a comprehensive analysis of the influence of intraseasonal surface wind anomalies on the continuous evolution of ENSO prediction.

[8] The data used in this study include the NCEP CFS real-time 9-month forecasts produced from February 2005 to January 2010 and the corresponding surface 10-meter zonal winds (U_{10m}) at the initial time from the NCEP/DOE Reanalysis-2 (R2) [*Kanamitsu et al.*, 2002]. The forecast data include two runs each day from February 2005 to December 2007 and four runs each day starting January 2008. The seasonal climatology for computing forecast anomalies is taken as the 1981–2004 average of retrospective forecast.

[9] To focus on the relationship between the forecasted anomalies and initial surface wind at the intraseasonal time scales, predicted anomalies at each lead time are band-pass filtered with respect to initial time. For the forecast of variable F at lead time τ from initial time t_0, total forecasted anomaly for each initial day, $F(t_0, \tau)$, is first calculated by averaging the two or four daily forecast members. An intraseasonal >(10–70-day) band-pass filter is then applied to the initial time (t_0) dimension of $F(t_0, \tau)$ to obtain forecast anomalies that vary at *intraseasonal* time scales with respect to *initial time* (IIT), $F^{IIT}(t_0, \tau)$. While the original anomalies of $F(t_0, \tau)$ contain variations with t_0 at all time scales, $F^{IIT}(t_0, \tau)$ represents intraseasonal components, separate from the low-frequency component of $F(t_0, \tau)$. $F^{IIT}(t_0, \tau)$ allows a clearer analysis of the coherence between intraseasonal variations in forecasts and intraseasonal variability in initial conditions. The intraseasonal band-pass filter is similarly applied to observed $U_{10m}(t_0)$ from R2 to derive its intraseasonal component, $U^{IIT}_{10m}(t_0)$.

3. Results

[10] As discussed in section 1, shown in Figure 1 are the variations in the amplitude of the forecasted Nino3.4 SST

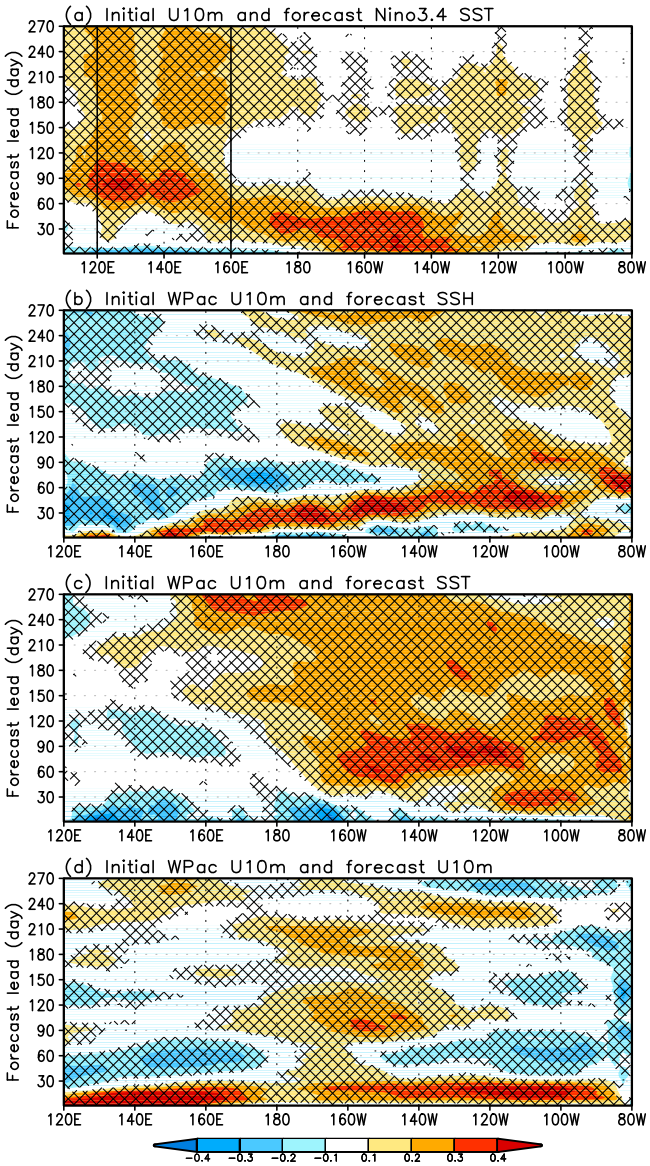

Figure 2. Lag correlations between IIT anomalies. (a) Initial 5°S–5°N average U_{10m} and forecasted Nino3.4 SST anomalies, (b) initial WPac (120°E–160°E/5°S–5°N average) U_{10m} and forecasted SSH,, (c) as in Figure 2b except for forecasted SST, and (d) as in Figure 2b except for U_{10m}. The vertical lines in Figure 2a indicate boundaries of longitudes used to define WPac U_{10m}. Hatchings indicate the significance level of 99% based on Monte Carlo approach whereby correlations after randomizing the initial U_{10m} are repeated 1000 times, and the significance is estimated based on the fraction of times the actual correlation exceeds correlations achieved with the randomized set.

index starting from initial dates between 1 November 2007 and 31 January 2008, a period of strong MJO activity. The intraseasonal component of the forecasted Nino3.4 SST and the observed U_{10m} in the WPac are given in Figures 1d and 1b respectively. The analysis in section 1 concluded that the amplitude of the predicted ENSO SST can vary substantially with the amplitude and the phase of surface winds at the initial time.

[11] Impacts of atmospheric intraseasonal variability (ISV) of WPac wind as in Figure 1 can also be seen during other periods. However, there are periods during which the WPac winds impacts were not as strong as those during the 2007/2008 winter. Further, atmospheric ISV in other regions may also have influence on the ENSO prediction. To assess the overall relationship between initial surface winds and forecasted SSTs, correlation between initial (i.e., observed) intraseasonal surface zonal winds $U^{IIT}_{10m}(t_0)$ of 5°S–5°N average and forecasted Nino3.4 SST IIT anomalies is calculated based on the forecasts from February 2005 to January 2010. Figure 2a shows that for lead time within 30 days, SST anomalies over the Nino3.4 region (170°W to 120°W; 5°S–5°N) are mostly correlated with local surface winds. For lead time beyond the 30 days, variations in Nino3.4 SST forecast are more closely related to remote surface winds that are located to the west of Nino3.4 region and progress systematically westward with increasing lead time. The correlation is highest at the lead time of about 80 days when the surface winds are located between 120E–150E.

[12] The connection between the western Pacific intraseasonal surface winds and intraseasonal Nino3.4 forecast is further explored by correlating the tropical (5°S–5°N average) sea surface height (SSH) and SST intraseasonal variations with tropical WPac $U^{IIT}_{10m}(t_0)$. Positive values of the WPac $U^{IIT}_{10m}(t_0)$ correlation with SSH are seen to propagate eastward from the western Pacific (Figure 2b), as a result of eastward propagating oceanic Kelvin waves induced by the intraseasonal surface winds in the western Pacific [*Kessler et al.*, 1995; *Hendon et al.*, 1998; *Seo and Xue*, 2005]. It takes about 60 days for the Kelvin waves to reach the eastern Pacific. Positive correlations remain in the central-eastern Pacific throughout most of the rest of forecast period, indicating the role of air-sea coupling in sustaining existing anomalies [*Latif et al.*, 1988; *Kessler and Kleeman*, 2000].

[13] At lead time within 30 days, SSTs in the western and central tropical Pacific are negatively correlated with the initial WPac surface zonal winds (Figure 2c), possibly due to enhanced evaporative cooling and vertical mixing [*Shinoda and Hendon*, 2001; *McPhaden*, 2002]. The correlation with SSTs becomes positive in most of the eastern Pacific around day 60 after the arrival of the oceanic Kelvin waves. It is interesting that positive correlation with SSTs start to appear near 112°W around day 15, well before the oceanic Kelvin waves propagate to the eastern Pacific. This positive correlation is possibly due to the direct impacts of the atmospheric forcing propagating from the western Pacific. This is confirmed in Figure 2d where surface wind U_{10m} propagates eastward and reaches the eastern Pacific within 30 days. The eastward propagating positive U_{10m} correlation during the beginning of the forecast is followed by eastward propagating negative correlation in the western Pacific and eastern Pacific, indicating the pair of the MJO westerly and easterly phases. The negative correlation in U_{10m} in the WPac is also consistent with the negative correlation in SSH (Figure 2b). The positive correlation in the central Pacific (around 160W) beyond 60-day lead time likely reflects the response of the atmosphere to SST anomalies (Figure 2c).

[14] The CFS has been shown to be comparable with other models in simulating the eastward propagation of the MJO, especially in low-level zonal wind [*Zhang et al.*,

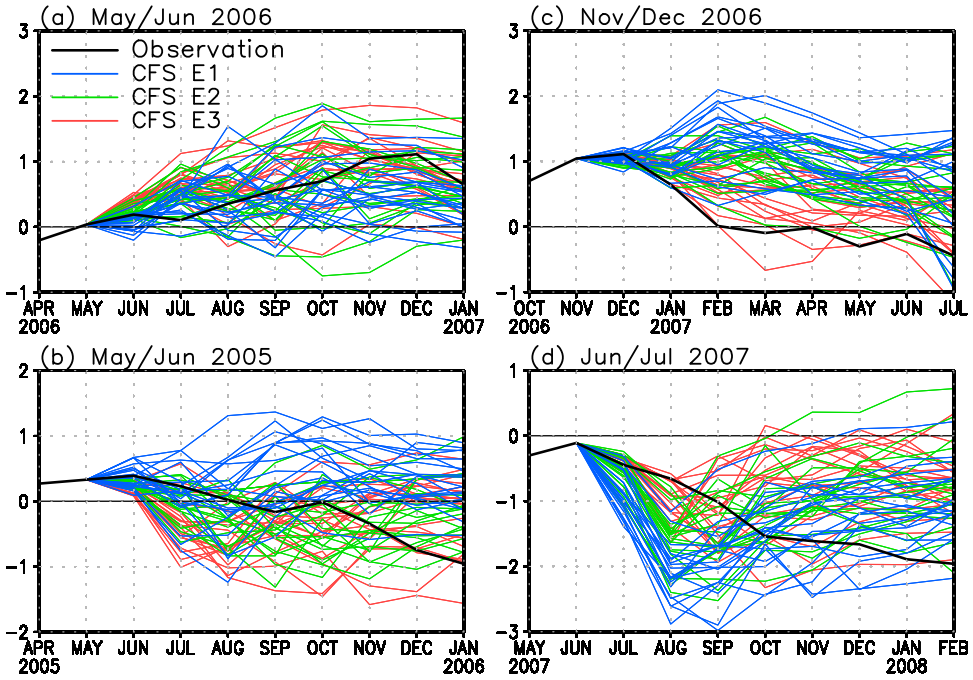

Figure 3. Examples of CFS forecasted Nino3.4 SST anomalies from initial conditions spanning 30 days. (a) Forecasts from May 12–21 (E1 in blue), May 22–31 (E2 in green), and June 1–10 2006 (E3 in red); (b) as in Figure 3a except for forecasts from May/June 2005; (c) as in Figure 3a except for forecasts from November/December 2006; and (d) as in Figure 3a except for forecast from June/July 2007. Observed anomalies are shown with black thick curves.

2006; *Kim et al.*, 2009; *Weaver et al.*, 2011]. However, in terms of prediction, the CFS is incapable of reproducing the observed MJO activities beyond 15–20 days as in the prediction with other methods [*Seo et al.*, 2009]. The fast eastward propagation of the initial atmospheric intraseasonal wind anomalies (Figure 2d) and the limit of predictability of atmospheric ISV indicate that the positive correlation in SSH (Figure 2b) and SST (Figure 2c) results primarily from the eastward propagation of the oceanic response to initial intraseasonal atmospheric forcing at the beginning of the forecast integration.

[15] For an ensemble of ENSO predictions initialized from daily observed initial conditions, individual forecast members diverge with lead time due to the growth of small differences in the initial conditions, and also due to the influence of the unpredictable stochastic atmospheric variability *during* the forecast target period. Because of their potential influence on SST variations in the eastern Pacific, differences in intraseasonal zonal wind anomalies in the WPac at initial times may lead to systematic intra-ensemble variations in the amplitude of predicted ENSO SSTs. For example, an ensemble of forecast members initialized across different stages of WPac wind anomalies may result in a wider spread of ENSO SST anomalies. Accordingly, the amplitude and probability distribution of the predicted ENSO SSTs can strongly depend on variations of strength and phase of intraseasonal zonal wind variability in the initial conditions.

[16] Examples of variations of forecasted Nino3.4 index with initial times are shown in Figure 3. Figures 3a–3d consist of forecasts for the same target seasons from 30 daily initial conditions spanning two months. Forecasts from the earliest (E1), second earliest (E2) and last 10 days (E3) are plotted with blue, green, and red colors. For example, for forecasts in Figure 3a from May–June 2006, E1 was from May 12–21, E2 from May 22–31, and E3 from

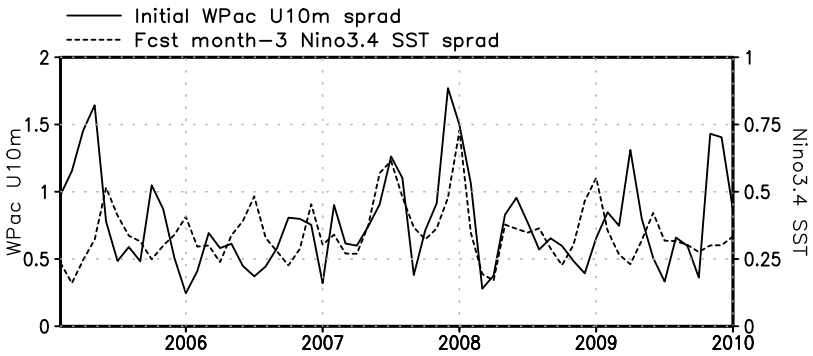

Figure 4. Spread of raw initial WPac U_{10m} spanning 30-initial days and corresponding spread of forecasted month-3 Nino3.4 SST raw anomalies.

Jun 1–10. The forecasts show a certain degree of separation among the three sets of 10-day initial periods, especially between E1 and E3 in the forecasts initialized from May/June 2005 (Figure 3b), November/December 2006 (Figure 3c), and June/July 2007 (Figure 3d). For example, forecasts in E3 (from 1–10 June 2005) are generally below normal while most of the forecasts in E1 (from 12–21 May 2005) are above normal (Figure 3b). These results indicate that ENSO forecasts can be substantially different even for initial conditions that are 10-day apart. These temporal variations of the ENSO forecast with initial time can be partially related to the changes in the initial state due to oceanic low-frequency dynamics as well as the perturbations to initial conditions resulting from atmospheric high-frequency variability.

[17] In a forecast system that uses a lagged ensemble consisting of forecasts initialized from daily initial conditions within a 30-day window, the probability distribution of the forecasted ENSO may depend on the variation of intraseasonal anomalies in the initial conditions. Figure 4 compares the spread of month-3 forecast of Nino3.4 SST raw anomalies among individual members initialized from a period of 30 days and the spread of the initial WPac daily-mean U_{10m}. It is shown that forecasted Nino3.4 SST spread is highly related to the variation in the initial zonal surface winds in the western Pacific during 2007 and 2008. The relationship of the spread is not as clear during other years, suggesting that other factors also contribute to the forecast ENSO probability.

4. Summary and Discussions

[18] This analysis shows how ENSO SST forecasts, for a fixed target period, but initialized from different initial times may depend on the influence of the initial surface wind anomalies. Forecast ensembles from initial conditions 10-day apart can be well separated, resulting in substantial differences in the forecasted ENSO amplitude. The variations, in part, result from the initial intraseasonal surface wind variability, especially that in the WPac. Strong WPac intraseasonal westerly (easterly) anomalies, such as those associated with MJO activity during November 2007 to January 2008, tends to lead to relatively warmer (colder) forecasted SST anomalies in the eastern Pacific by inducing subsurface oceanic Kelvin waves in the western Pacific that propagate eastward and arrive at the eastern Pacific in about 60 days. In addition, forecast ensembles that consist of individual members initialized from a period of strong intraseasonal variability may also result in a larger forecast ensemble spread.

[19] One implication of these results is that the initial intraseasonal variability must be taken into account in the interpretation of the forecasted ENSO amplitude and predictability of individual ENSO events. Forecasts from a stage of strong westerly surface wind anomalies in the western Pacific would result in a higher probability of warmer Nino3.4 SSTs. Such an impact by initial stage of surface winds is of critical importance in operational forecasts. For example, the National Oceanic and Atmospheric Administration uses a threshold of ±0.5 K to categorize ENSO event and a few tenths of degree differences in Nino3.4 SST forecast may result in an observed outcome different from the outlook. Since the observed ENSO evolution is impacted by initial intraseasonal anomalies as well as atmospheric stochastic forcings during the forecast period, predictability of ENSO relies on the extent to which the low-frequency ENSO dynamics is impacted by initial intraseasonal anomalies as well as observed stochastic forcings.

[20] Another implication of the results discussed here is the design of coupled seasonal prediction systems. Two types of ensemble configurations are currently being used for operational ENSO forecasts. In the first type, the "burst ensemble", all forecasts are produced at a certain date from initial conditions with perturbations to the atmospheric and oceanic states [*Anderson et al.*, 2007]. In the second type, the "lagged ensemble", a set of forecasts is initialized every day and forecasts spanning a certain number of initial days are used to form the ensemble [*Alves et al.*, 2003; *Saha et al.*, 2006].

[21] Our study suggests that the characteristics of these two types of ensembles may be different when the observed initial conditions contain large intraseasonal variability. If the *observed* intraseasonal variation is *weak at the initial time*, a burst ensemble and a lagged ensemble may lead to similar ENSO predictions. On the other hand, if there exists strong intraseasonal activity at the initial time, a burst ensemble initialized at a particular interval (e.g., once a month) without sufficient perturbations to represent the spread of observed strong intraseasonal anomalies may result in a forecast bias corresponding to the specific initial time, while a lagged ensemble may lead to a wide range of intra-member spread.

[22] Our analysis is based on forecasts for a relatively short period. While such a data set allows an analysis of the causes of the continuous evolution of predicted El Niño SSTs, longer history of forecast data are required to analyze other aspects of ENSO prediction. For example, the seasonal dependence of the impacts of the initial intraseasonal activities on the ENSO forecast has not been well explored. The variability associated with both ENSO and the MJO, the dominant modes at interannual and intraseasonal time scales, has strong seasonality. It is possible that the influence of the intraseasonal activities on the ENSO forecast is different during different seasons. In addition, most of previous studies have focused on the impacts of WWEs on El Niño events. Our results indicate that both westerly and easterly anomalies influence the ENSO evolution. The relative role of the intraseasonal variability on the prediction of different ENSO phases is unclear, and needs to be further analyzed. Further, coupled forecast experiments from identical oceanic initial conditions but with the inclusion and exclusion of intraseasonal wind forcing will help quantify its contribution to ENSO amplitude and spread.

[23] **Acknowledgments.** The Editor thanks the anonymous reviewer for their assistance in evaluating this paper.

References

Alves, O., et al. (2003), POAMA: Bureau of Meteorology operational coupled model seasonal forecast system, in *Science for Drought: Proceedings of the National Drought Forum, Brisbane, April 2003*, edited by R. Stone and I. Partridge, pp. 49–56, Dep. of Primary Ind., Brisbane, Queensl., Australia.

Anderson, D., T. Stockdale, M. Balmaseda, L. Ferranti, F. Vitart, F. Molteni, F. J. Doblas-Reyes, K. Mogensen, and A. Vidard (2007), Development of the ECMWF seasonal forecast system 3, *ECMWF Tech. Memo. 503*, 56 pp., Eur. Cent. for Medium-Range Weather Forecasts, Reading, U. K.

Barnston, A. G., M. H. Glantz, and Y. He (1999), Predictive skill of statistical and dynamical climate models in SST forecasts during the 1997–98 El Niño episode and the 1998 La Niña onset, *Bull. Am. Meteorol. Soc.*, *80*, 217–243, doi:10.1175/1520-0477(1999)080<0217:PSOSAD>2.0.CO;2.

Batstone, C., and H. H. Hendon (2005), Characteristics of stochastic variability associated with ENSO and role of MJO, *J. Clim.*, *18*, 1773–1789, doi:10.1175/JCLI3374.1.

Eisenman, I., L. Yu, and E. Tziperman (2005), Westerly wind bursts: ENSO's tail rather than the dog?, *J. Clim.*, *18*, 5224–5238, doi:10.1175/JCLI3588.1.

Hendon, H. H., B. Liebmann, and J. D. Glick (1998), Oceanic Kelvin waves and the Madden–Julian Oscillation, *J. Atmos. Sci.*, *55*, 88–101, doi:10.1175/1520-0469(1998)055<0088:OKWATM>2.0.CO;2.

Kanamitsu, M., W. Ebisuzaki, J. Woollen, S.-K. Yang, J. J. Hnilo, M. Fiorino, and G. L. Potter (2002), NCEP-DEO AMIP-II reanalysis (R-2), *Bull. Am. Meteorol. Soc.*, *83*, 1631–1643, doi:10.1175/BAMS-83-11-1631

Kessler, W. S., and R. Kleeman (2000), Rectification of the Madden–Julian Oscillation into the ENSO Cycle, *J. Clim.*, *13*, 3560–3575, doi:10.1175/1520-0442(2000)013<3560:ROTMJO>2.0.CO;2.

Kessler, W. S., M. J. McPhaden, and K. M. Weickmann (1995), Forcing of intraseasonal Kelvin waves in the equatorial Pacific, *J. Geophys. Res.*, *100*(C6), 10,613–10,631.doi:10.1029/95JC00382

Kim, D., et al. (2009), Application of MJO simulation diagnostics to climate models, *J. Clim.*, *22*, 6413–6436.doi:10.1175/2009JCLI3063.1

Latif, M., J. Biercamp, and H. Von Storch (1988), The response of a coupled ocean-atmosphere general circulation model to wind bursts, *J. Atmos. Sci.*, *45*, 964–979, doi:10.1175/1520-0469(1988)045<0964:TROACO>2.0.CO;2.

McPhaden, M. J. (2002), Mixed layer temperature balance on intraseasonal timescales in the equatorial Pacific Ocean, *J. Clim.*, *15*, 2632–2647, doi:10.1175/1520-0442(2002)015<2632:MLTBOI>2.0.CO;2.

McPhaden, M. J. (2008), Evolution of the 2006–2007 El Niño: The role of intraseasonal to interannual time scale dynamics, *Adv. Geosci.*, *14*, 219–230, doi:10.5194/adgeo-14-219-2008.

McPhaden, M. J., X. Zhang, H. H. Hendon, and M. C. Wheeler (2006), Large scale dynamics and MJO forcing of ENSO variability, *Geophys. Res. Lett.*, *33*, L16702, doi:10.1029/2006GL026786.

Picaut, J., M. Ioualalen, C. Menkes, T. Delcroix, and M. J. McPhaden (1996), Mechanism of the zonal displacements of the Pacific warm pool: Implications for ENSO, *Science*, *274*, 1486–1489, doi:10.1126/science.274.5292.1486.

Saha, S., et al. (2006), The NCEP Climate Forecast System, *J. Clim.*, *19*, 3483–3517, doi:10.1175/JCLI3812.1.

Seiki, A., and Y. N. Takayabu (2007), Westerly wind bursts and their relationship with intraseasonal variations and ENSO. Part I: Statistics, *Mon. Weather Rev.*, *135*, 3325–3345, doi:10.1175/MWR3477.1.

Seo, K.-H., and Y. Xue (2005), MJO-related oceanic Kelvin waves and the ENSO cycle: A study with the NCEP Global Ocean Data Assimilation System, *Geophys. Res. Lett.*, *32*, L07712, doi:10.1029/2005GL022511.

Seo, K.-H., W. Wang, J. Gottschalck, Q. Zhang, J.-K. E. Schemm, W. R. Higgins, and A. Kumar (2009), Evaluation of MJO forecast skill from several statistical and dynamical forecast models, *J. Clim.*, *22*, 2372–2388, doi:10.1175/2008JCLI2421.1.

Shi, L., O. Alves, H. H. Hendon, G. Wang, and D. Anderson (2009), The role of stochastic forcing in ensemble forecasts of the 1997/98 El Niño, *J. Clim.*, *22*, 2526–2540, doi:10.1175/2008JCLI2469.1.

Shi, L., H. H. Hendon, O. Alves, M. C. Wheeler, D. Anderson, and G. Wang (2010), On the importance of initializing the stochastic part of the atmosphere for forecasting the 1997/1998 El Niño, *Clim. Dyn.*, doi:10.1007/s00382-010-0933-9.

Shinoda, T., and H. H. Hendon (2001), Upper-ocean heat budget in response to the Madden–Julian oscillation in the western equatorial Pacific, *J. Clim.*, *14*, 4147–4165, doi:10.1175/1520-0442(2001)014<4147:UOHBIR>2.0.CO;2.

Vecchi, G. A., and D. E. Harrison (2000), Tropical Pacific sea surface temperature anomalies, El Niño, and equatorial westerly wind events, *J. Clim.*, *13*, 1814–1830, doi:10.1175/1520-0442(2000)013<1814:TPSSTA>2.0.CO;2.

Vitart, F., M. A. Balmaseda, L. Ferranti, and D. Anderson (2003), Westerly wind events and the 1997/98 El Niño event in the ECMWF seasonal forecasting system: A case study, *J. Clim.*, *16*, 3153–3170, doi:10.1175/1520-0442(2003)016<3153:WWEATE>2.0.CO;2.

Weaver, S. J., W. Wang, M. Chen, and A. Kumar (2011), Representation of MJO variability in the NCEP Climate Forecast System, *J. Clim.*, doi:10.1175/2011JCLI4188.1.

Zhang, C., and J. Gottschalck (2002), SST Anomalies of ENSO and the Madden–Julian Oscillation in the equatorial Pacific, *J. Clim.*, *15*, 2429–2445, doi:10.1175/1520-0442(2002)015<2429:SAOEAT>2.0.CO;2.

Zhang, C., et al. (2006), Simulations of the Madden-Julian Oscillation in four pairs of coupled and uncoupled global models, *Clim. Dyn.*, *27*, 573–592.doi:10.1007/s00382-006-0148-2

M. Chen, A. Kumar, W. Wang, and Y. Xue, Climate Prediction Center, NCEP, NWS, NOAA, 5200 Auth Rd., Camp Springs, MD 20746, USA. (wanqiu.wang@noaa.gov)